Removal of Nitrogen Monoxide through a Novel Catalytic Process. 2. Infrared Study on Surface Reaction of Nitrogen Monoxide Adsorbed on Copper Ion-Exchanged ZSM-5 Zeolites

Masakazu Iwamoto,* Hidenori Yahiro, Noritaka Mizuno, Wen-Xiang Zhang, Yoshihiro Mine,† Hiroshi Furukawa,† and Shuichi Kagawa†

Catalysis Research Center, Hokkaido University, Sapporo 060, Japan (Received: December 2, 1991)

Infrared spectroscopy combined with an isotropic tracer method has been used to study the adsorption of NO over copper ion-exchanged ZSM-5 zeolites and to elucidate the reaction mechanism of catalytic decomposition of NO. Three distinct states of adsorbed NO have been detected, being attributed to $NO^{\delta+}$, $NO^{\delta-}$, and $(NO)_2^{\delta-}$. The intensities of 1827- and 1734-cm^{-1} bands, symmetric and asymmetric stretching vibration of the dimer species, respectively, concluded that the bond angle ON-Cu-NO in $(NO)_2^{\delta-}$ is 103°. The IR experiments on evacuated, oxidized, or CO-preadsorbed copper ion-exchanged ZSM-5 zeolites and ESR or phosphorescence measurements indicated that $NO^{\delta-}$ and $(NO)_2^{\delta-}$ are formed on copper(I) ions while $NO^{\delta+}$ on copper(II) ions. The formation of the anionic species depended on the partial pressure of NO, $NO^{\delta-}$(ads) + NO(gas) → $(NO)_2^{\delta-}$(ads). The intensities of the infrared bands attributable to $NO^{\delta-}$ and $(NO)_2^{\delta-}$ decreased at ambient temperature with reaction time, while that of $NO^{\delta+}$ increased. The change of the distribution of products in the gas phase with adsorption time was measured and the formation of N_2 and N_2O was confirmed even at room temperature on the evacuated sample. It follows that the Cu^+ ions are active centers, $NO^{\delta-}$ and/or $(NO)_2^{\delta-}$ species are intermediates for the decomposition of NO over copper ion-exchanged ZSM-5 zeolite catalyst, and the catalytic reaction cycle proceeds at or above 573 K, at which oxygen generated through the decomposition can desorb.

Introduction

Copper ion-exchanged zeolites, in particular copper ion-exchanged ZSM-5 zeolites, have been reported to be active for catalytic decomposition of nitrogen monoxide (NO).[1-3] These findings and stoichiometry of the reaction were further confirmed by Li and Hall.[4] Since catalytic decomposition of NO is the simplest and most desirable method for the removal of NO from exhaust streams and Cu-zeolites are the most suitable for the reaction among the catalysts reported,[5-8] clarifying the state of NO adsorbed, the interaction of NO with copper ion, and the reaction mechanism is remarkably important for progress in the chemistry of NO decomposition and design of the decomposition catalyst. In the present work, they are studied by infrared spectroscopy.

Infrared studies of nitrosyl complexes[9] and NO adsorbed on solid catalysts[10-17] have widely been reported. NO contains one electron in the antibonding $2p\pi^*$ orbital. It is well-known that NO^+ is produced by donation of the electron from the antibonding orbital of NO to a d orbital of metal and NO^- by transfer of a d electron of the metal to the antibonding orbital of NO. The bond strength of NO in each species is stronger or weaker than that in a neutral NO. A large number of reports are concerned with these species on solid catalysts; for example, Arai and Tominaga[10] confirmed Rh-NO^+ and Rh-NO^- on alumina, and complexes of NO with Cr^{2+}, Fe^{2+}, Co^{2+}, Ni^{2+}, and Cu^{2+} ions in Y-type zeolite were also reported.[18-22] These papers, however, have dealt with the complex formation or reduction mechanism of NO with ammonia or CO and there is no report on the decomposition mechanism except fundamental studies on clean metal surfaces[23] or metal/support at higher temperatures.[14,24]

Recently, it has been found that repeated ion exchange of ZSM-5 zeolite with Cu^{2+} solution resulted in excess loadings of copper ions above 100% exchange level and the resulting catalysts were more active for the decomposition of NO than the catalyst with exchange level of copper ion below 100%.[2] In the IR experiments, we have briefly reported on the copper ion-exchanged ZSM-5 zeolite with 50-80% ion-exchange level, that NO could be adsorbed as NO^+, NO^-, and $(NO)_2^-$ species, and that the anionic species decreased with adsorption time whereas NO^+ increased.[25] However, on the excessively copper ion-exchanged ZSM-5 zeolites little is known of the adsorbed NO species, the state of adsorption sites, and reaction mechanism for decomposition of NO. In this paper, adsorbed species of NO on excessively copper ion-exchanged ZSM-5 zeolite were confirmed by using an isotopic tracer method, adsorption sites for the respective adsorbates were determined by several techniques, and finally time-resolved IR spectra were measured in a sequential fashion to reveal the reaction mechanism.

Experimental Section

The copper ion-exchanged ZSM-5 zeolites were prepared at room temperature by the method previously reported.[2] The amount of Al in the parent ZSM-5 measured by a Si MAS NMR method[26] was 7.6 atoms/unit cell. Approximately 15 g of the sodium ion-exchanged ZSM-5 zeolite supplied by Tosoh Corp. was washed with dilute $NaNO_3$ solution and ion-exchanged in 1 dm^3 of the copper(II) acetate solution with 10-11 mmol dm^{-3} overnight. The wet cake obtained by filtration was again ion-exchanged in new copper(II) acetate solution. After the desired repetition of the ion-exchange treatment, the sample was washed and dried at 383 K. The amount of copper ions exchanged was determined by atomic absorption spectroscopy after the zeolite sample obtained was dissolved in HF solution. The exchange level of copper in zeolite was calculated by 2(amount of Cu)/(amount of Al). Several copper ion-exchanged ZSM-5 zeolites having exchange levels of copper ion of 18-157% (0.7-6.0 Cu ions/unit cell) were used. Hereafter, the sample was abbreviated as Cu-MFI-157 (cation-zeolite structure-exchange level).

Infrared spectra were collected by using an IR-810 spectrometer (Japan Spectroscopic Co., Ltd.) and a quartz infrared cell with CaF_2 window similar to that described elsewhere.[27] The volume of the quartz infrared cell is 309 cm^3. A self-supporting zeolite wafer (20-30 mg, 3 cm^2) was prepared by pressing powder under a pressure of 300 kg cm^{-2} for 30 min. The infrared spectra were measured in the region 4000-900 cm^{-1} at an ambient temperature, 5 min after various treatments unless otherwise stated. Intensities of absorption bands, I_{1813}, were determined by the peak area measured in an absorbance mode, where the subscript is wavenumber of the IR band. The standard pretreatment was as follows: the sample was heated to 773 K under vacuum, evacuated for 30 min, exposed to oxygen (P_{O_2} = 100 Torr, 1 Torr = 0.133 kPa),

* Address correspondence to this author at the Catalysis Research Center, Hokkaido University, Sapporo 060, Japan.
† Department of Industrial Chemistry, Faculty of Engineering, Nagasaki University, Nagasaki 851, Japan.

0022-3654/92/2096-9360$03.00/0

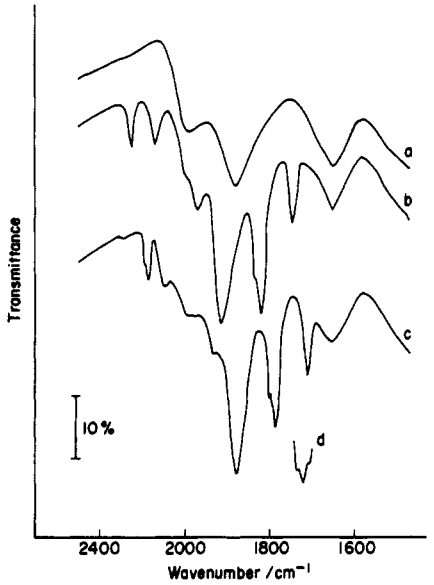

Figure 1. Infrared spectra of Cu-MFI-81: (a) Background spectrum. (b) Exposure to ^{14}NO (18.2 Torr). (c) Exposure to ^{15}NO (18.5 Torr). (d) Exposure to ^{14}NO (9.0 Torr) + ^{15}NO (9.0 Torr).

TABLE I: Infrared Bands of NO Adsorbed on Cu-MFI-81 and Their Assignments

frequencies/cm^{-1}			
obsd in Figure 1b	obsd in Figure 1c	calcd by eq 1	assignment
2238	2170	2198 (2162)[a]	$\nu(N_2O)$
2125	2087	2087	$\nu(NO_2^+)$
1964	1927	1929	$\nu(NO)^{\delta+}$ adsorbed on $(Cu)_n$
1906	1874	1872	$\nu(NO)^{\delta+}$
1827	1795	1794	symmetric $\nu(NO)_2^{\delta-}$
1813	1781	1781	$\nu(NO)^{\delta-}$
1734	1703	1703	asymmetric $\nu(NO)_2^{\delta-}$

[a] The value was calculated by assuming that the band is assigned to the ^{15}N–^{15}N stretching vibration.

evacuated again for 30 min, and then cooled down to a desired temperature. This was performed to remove such impurities on the zeolite surface as water, carbon dioxide, and oxygen. The maximum transmittance for each sample was approximately 50% after this pretreatment.

Reactivity of the pretreated Cu-zeolite with NO at room temperature was measured with a fixed-bed flow reactor. The Cu-MFI-130 (1.0 g) placed in the reactor was heated at 773 K for 2 h under a He stream (30 cm^3 min^{-1}). The concentration of NO was 1.0% and the balance was helium. The total flow rate was 15 cm^3 min^{-1}. The gas composition was analyzed by gas chromatography using Porapak Q (N_2O) and Molecular Sieve 5A (N_2, O_2, and NO) columns.

Results

Infrared Spectra of NO Adsorbed. Figure 1 shows the infrared spectra of NO adsorbed on Cu-MFI-81. Curve a is the background, i.e., the spectrum of the zeolite itself after the standard pretreatment. Upon admission of ^{14}NO (18.2 Torr) seven peaks were observed in the range 2500–1500 cm^{-1} (Figure 1b): six intense bands at 2238, 2125, 1964, 1906, 1813, and 1734 cm^{-1} and a shoulder at 1827 cm^{-1}. These spectra changed with adsorption time, which will be mentioned in the later section. Additional infrared bands were detected below 1500 cm^{-1}, but they were not clear because of the intense bands of the CaF_2 window.

Figure 1c shows the infrared spectrum after ^{15}NO adsorption on Cu-MFI-81. The spectrum was essentially the same as that of Figure 1b, except that all bands were shifted to the respective lower wavenumbers (2170, 2087, 1927, 1874, 1795, 1781, and 1703 cm^{-1}). The bands observed after exposure to ^{14}NO or ^{15}NO are summarized in Table I. When Cu-MFI-81 was exposed to an equimolar mixture of ^{14}NO and ^{15}NO, a very complicated spectrum was observed. Most of the peaks corresponded with those in either part a or b of Figure 1, and it was found that a new band appeared at 1719 cm^{-1} (Figure 1d). I_{1734}, I_{1719}, and I_{1703} were approximately in the ratio 1:2:1.

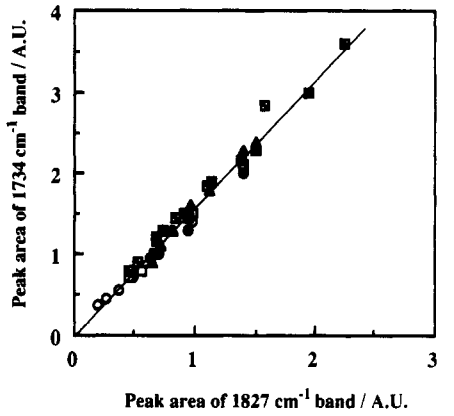

Figure 2. Correlation between peak areas of 1827- and 1734-cm^{-1} bands. Cu-MFI-122: ○, P_{NO} = 141.1 Torr; ●, 81.2 Torr; □, 39.9 Torr; ■, 40.1 Torr; △, 39.4 Torr. Cu-MFI-93: ▲, 77.2 Torr; ▣, 40.0 Torr. Cu-MFI-48: ▣, 39.9 Torr.

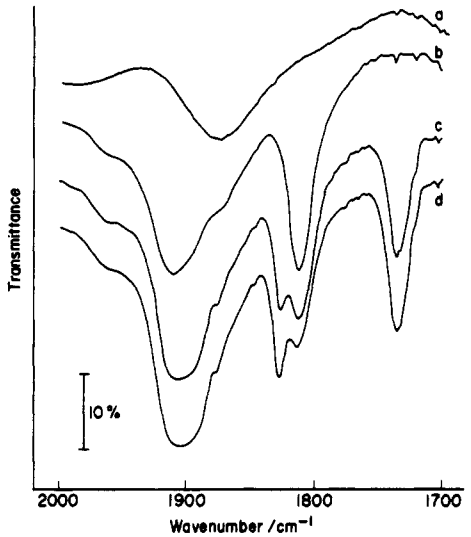

Figure 3. Infrared spectra after addition of ^{14}NO at pressure of (a) 0.0 (background), (b) 1.3, (c) 39.9, and (d) 81.2 Torr on Cu-MFI-112.

To get more information on the adsorbates the change of the peak intensities with the ion-exchange level and partial pressure of NO was measured. A clear correlation was found between I_{1827} and I_{1734} as plotted in Figure 2. It is evident that the ratio of I_{1734} to I_{1827} is always kept constant at 1.60, regardless of the variation of copper contents or NO pressures.

It would be worthy to note that the bands at 1827, 1813, and 1734 cm^{-1} disappeared after brief evacuation even at room temperature. In contrast, the band at 1906 cm^{-1} was gradually eliminated by the evacuation at room temperature, suggesting that the desorption of the corresponding adsorbed species is an activated process.

Adsorption Sites for NO. It was confirmed that the NO species observed in Figure 1 adsorb on copper ions exchanged into zeolite, since no absorption band attributable to adsorbed species of NO was observed on Na-MFI-100.

Pretreatment of Cu-MFI before the NO adsorption affected the adsorption state of NO. After the sample was pretreated by the standard procedure and cooled down to room temperature before 773 K in an oxygen atmosphere (P_{O_2} = 100 Torr), the introduction of ^{14}NO resulted in the appearance of an absorption band at 1906 cm^{-1} but hardly yielded the bands at 2238, 2125,

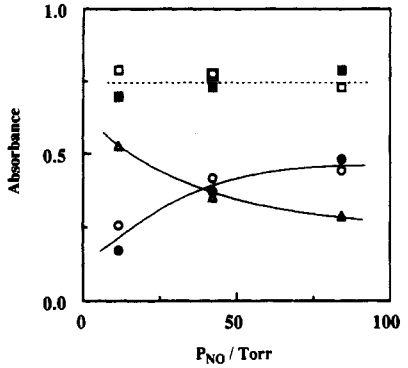

Figure 4. NO pressure dependence of absorbances of the bands at (△) 1813, (○) 1827, and (●) 1734 cm^{-1}. □, ■, and the dashed line indicate the sums of △ and ○, △ and ●, and solid lines, respectively. Catalyst, Cu-MFI-112.

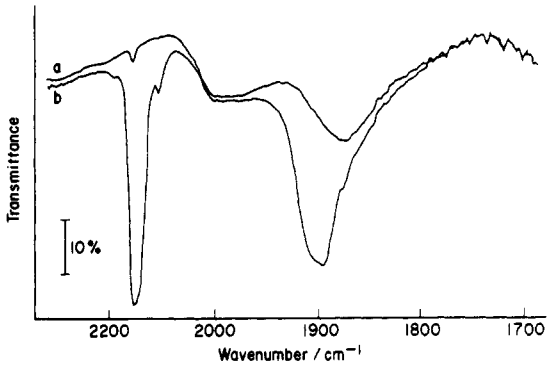

Figure 5. Infrared spectra of Cu-MFI-130: (a) Background spectrum. (b) Adsorption of ^{14}NO (36.8 Torr) after the preadsorption of CO (121.5 Torr).

1964, 1827, 1813, and 1734 cm^{-1}. On this sample, there was no change in the band intensity with time. When the same sample was evaluated at 773 K, the admittance of ^{14}NO caused an infrared spectrum including the bands at 1827, 1813, and 1734 cm^{-1}, which was essentially the same as that of Figure 1b.

Figure 3 shows the dependence of the infrared spectra of ^{14}NO adsorbed on Cu-MFI-112 on the pressure of ^{14}NO. The bands at 1827 and 1734 cm^{-1} could not be detected at the NO pressure of 1.3 Torr and increased with increment of NO pressure. By contrast, the band at 1813 cm^{-1} decreased with increasing the pressure of NO. The intensity of the band at 1906 cm^{-1} increased a little with the increment of the NO pressure.

Based on the results in Figure 3, the dependency of I_{1827}, I_{1813}, and I_{1734} on the NO pressure is depicted in Figure 4. Clearly I_{1827} and I_{1734} increased with the increment of the pressure of NO, while I_{1813} decreased. It should be noted here that the sum of I_{1813} and I_{1734} (or I_{1813} and I_{1827}) was constant, independent of NO pressure.

At last the effect of CO preadsorption on the NO adsorption was examined. After CO was introduced at room temperature and P_{CO} = 121.5 Torr for 5 min on Cu-MFI-130 pretreated and was removed by evacuation, 36.8 Torr of ^{14}NO was admitted. In the IR measurement, intense bands appeared at 2154 and 1896 cm^{-1} as shown in Figure 5, while no band was detected at 1827, 1813, and 1734 cm^{-1} on the CO-preadsorbed Cu-MFI-130.

Dynamic Change in Infrared Spectra of NO Adsorbed. We have reported that the intensities of infrared bands changed greatly with adsorption time when NO was adsorbed on Cu-MFI-81 subjected to the standard pretreatment.[25] In this study, the variation on Cu-MFI-112, which was more active than Cu-MFI-81 for the decomposition of NO,[3] is depicted in Figure 6. I_{1827}, I_{1813}, I_{1964}, and I_{1734} decreased with adsorption time. On the other hand, I_{2125} and I_{1906} increased and no change of I_{2238} was observed. Similar spectra and variation in peak intensities with time were observed for Cu-MFI having the exchange level of copper ion in the region 18–157%.

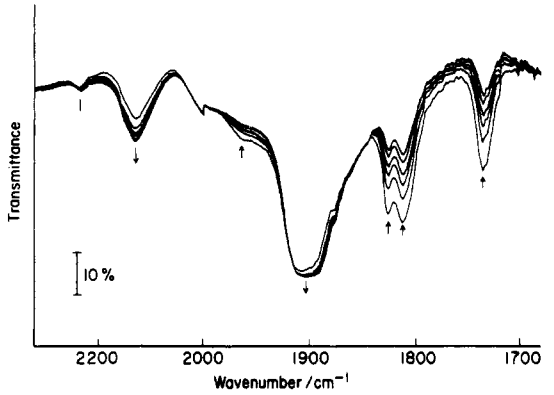

Figure 6. Infrared spectra of Cu-MFI-112 after the addition of NO (39.9 Torr) for 4, 13, 27, 45, and 66 min. The upward and downward arrows indicate decrease and increase in the peak intensities with time, respectively.

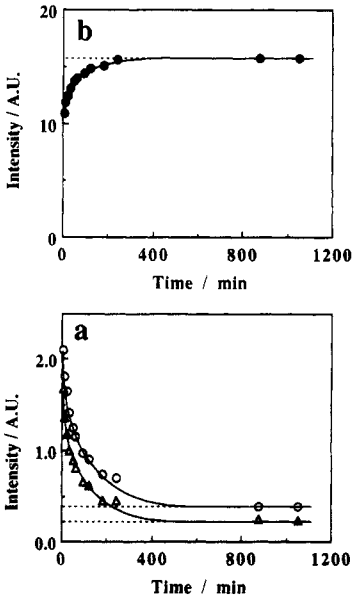

Figure 7. Time dependence of intensity of the bands at (a, ○) 1813, (a, △) 1734, and (b, ●) 1906 cm^{-1} after the introduction of 52 Torr of NO. Catalyst, Cu-MFI-157.

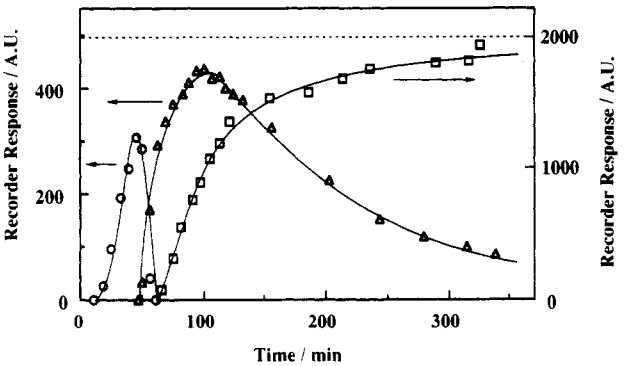

Figure 8. Time course of distribution of effluents from reaction with Cu-MFI-130 (1.0 g) at 4.0 g s cm^{-3}, P_{NO} = 1.0%, and room temperature. ○, N_2; △, N_2O; □, NO. The dashed line indicates the concentration of NO at the inlet of the reactor.

Figure 7a shows the changes in the intensities of the bands at 1813 and 1734 cm^{-1} when Cu-MFI-157 was exposed to 52 Torr of NO. Both intensities sharply decreased at first and reached constant values after 870 min. In contrast, the intensity of the band at 1906 cm^{-1} increased and also reached a constant value after 870 min, as shown in Figure 7b.

Decomposition of NO on Cu-MFI at Room Temperature. To determine products in the gas phase during the above IR mea-

surements, we first attempted to detect them directly by gas chromatography. No success, however, was obtained owing to too small amounts of the products. Here the change in distribution of products was measured in a flow system. The time course of product distribution over pretreated Cu-MFI-130 at room temperature is shown in Figure 8, where NO/He mixture flowed continuously. Just after the admittance of NO, no product and no NO were observed, showing that NO or decomposition products were completely adsorbed. Evolution or production of N_2 started after ca. 12 min, was maximized after 45 min, and diminished after 60 min. N_2O was observed to come out after 45 min. The amount was increased with reaction time, reached a maximum after 100 min, and then decreased gradually. NO was detected 60 min after NO admittance and increased gradually with reaction time. After 300 min the concentration of NO at the outlet of reactor became close to that at the inlet. The amounts of N_2 and N_2O produced during the experiment of Figure 8 were 0.46 and 0.02 mol/mol of Cu, respectively.

It was confirmed in a separate experiment that the admission of NO on oxidized or CO-preadsorbed zeolite gave a very small amount of N_2 or N_2O.

Discussion

Adsorbed Species of NO on Cu-MFI. It should first be discussed whether the additional absorption bands detected below 1500 cm^{-1}, which could not be measured clearly, are essentially important in the discussion concerning the decomposition mechanism or not. On the basis of previous results,[10-22] these bands can be assigned to NO_2 or NO_3 species with a certain negative charge. These species would be produced through the disproportionation of NO molecules or through the reaction of NO with oxygen atoms generated in the decomposition reaction. Since it is scarcely possible to consider that they are intermediates in the decomposition of NO, no further consideration was given here to these adsorbed species.

In order to assign each absorption band, studies on the adsorption of isotopically substituted NO on the Cu-MFI sample were carried out. It could readily be observed in the presence of pure ^{15}NO that all bands depicted in Figure 1b were shifted to the respective lower wavenumbers. The frequency of stretching vibration of ^{15}NO, ν_{15}, can be calculated by the following equation using that of ^{14}NO, ν_{14}:[28]

$$\nu_{15} = \nu_{14}(\mu_{14}/\mu_{15}) \quad (1)$$

where μ_{14} is the reduced mass for ^{14}N and ^{16}O and μ_{15} the reduced mass for ^{15}N and ^{16}O. The values of ν_{15}'s thus estimated are summarized in Table I. They agreed well with the observed values except for the band at 2238 cm^{-1}. The large isotope shift of the band at 2238 cm^{-1} can be explained by assuming that two ^{15}N's are incorporated in the molecule adsorbed. The calculated value for the stretching vibration of two ^{15}N's was 2162 cm^{-1}, which agreed approximately with the observed one. Therefore, this band would be assigned to a N–N stretching vibration.

The 1:1 mixture system provided conclusive evidence for the dinitrosyl adsorbate. We observed a new band at 1719 cm^{-1} after introduction of the mixture of ^{14}NO and ^{15}NO and the relative intensities for the three peaks at 1734, 1719, and 1703 cm^{-1} were approximately in the ratio 1:2:1 (Figure 1d). The results indicate the presence of a $Cu(^{14}NO)(^{15}NO)$ adsorbate and confirm the assignment of the band at 1734 cm^{-1} in Figure 1b to the dinitrosyl species. In a similar way, $[Co(NO)_2]$ complex in Y-type zeolite has been confirmed by Windhorst and Lunsford.[20] It was expected in this experiment that a new band would appear between 1827 and 1795 cm^{-1} due to the $Cu(^{14}NO)(^{15}NO)$ species. Unfortunately, we could not observe any new band with clear resolution in this region because of overlapping of the Cu–NO bands at 1813 and 1781 cm^{-1}.

The above assignment was further confirmed by the linear correlation shown in Figure 2. The linear correlation or constant ratio between I_{1827} and I_{1734} indicates that the above assignments are reasonable and the angle between two NO molecules is constant irrespective of the change in the ion-exchange level or the partial pressure of NO. It is well-known that the stretching vibration of dinitrosyl adsorbates was divided into symmetric and asymmetric bands. Taking into consideration the dipolar interactions and the infrared spectra reported by Dinerman and Ewing,[29] the 1827- and 1734-cm^{-1} bands correspond to symmetric and asymmetric stretching vibration, respectively. The relative intensity of the two bands at 1827 (I_{1827}) and 1734 cm^{-1} (I_{1734}) is related to the angle (2θ) between the two N–O oscillators:[30]

$$2\theta = 2 \arctan (I_{1827}/I_{1734})^{0.5} \quad (2)$$

An invariant ratio of the doublet peaks existed in the present experiments and was 1.60 as shown in Figure 2, which indicates that the angle is approximately 103°. This value can be compared with those of related dinitrosyl species adsorbed on different active centers (Table II). The reported angles were, for example, 120° on Rh–alumina,[33] 123° on Co–Y zeolites,[20] and 116–97° on molybdena–alumina.[16,34,35] The value observed on Cu-MFI is included in the range of angles reported so far.

The band wavenumber of 1813 cm^{-1} is lower than that of gaseous NO molecule (1876 cm^{-1}). The shift to lower wavenumber is observed when the NO adsorbed is anionic.[10,36] The band at 1813 cm^{-1} falls within the range assigned to the $NO^{\delta-}$ stretching vibration. As shown in Figure 4, the intensities of the infrared bands at 1813 and 1734 (or 1827) cm^{-1} changed in a complementary way with NO pressure and their sum remained constant. This result indicates that the $NO^{\delta-}$ species and the dinitrosyl species are adsorbed on the same sites and the ratio is dependent on the NO pressure and that the dinitrosyl adsorbates should be anionic, i.e., $(NO)_2^{\delta-}$, because the reaction $NO^{\delta-}(ads) + NO(gas) \rightarrow (NO)_2^{\delta-}(ads)$ proceeds under higher pressures of NO. These assignments will be further substantiated in the discussion of adsorption sites. It should be noted that the two bands at 1827 and 1734 cm^{-1} were assigned to an *anionic* dinitrosyl species, and earlier investigators[20,22,37] did not detect these features on copper ion-exchanged zeolites.

To confirm the assignment of the anionic dinitrosyl species we compare the present result with the related dinitrosyl species adsorbed on different sites listed in Table II. One can find that the present values of 1827 and 1734 cm^{-1} are rather low and close to those on reduced MoO_3/Al_2O_3 samples.[16,34,35] On the sample the $(NO)_2$ species were reported to be formed only on reduced Mo sites.[16,34,35] In the Co/Y system the coadsorption of ammonia (an electron-donating substrate) on Co resulted in the lowering of the dinitrosyl bands.[20] By contrast, the Rh/Y,[31,32] Fe/Y,[19] Co/Y,[20] and Cr/SiO_2[38] systems gave the peaks at 1850–1920 and 1745–1830 cm^{-1}, indicating that the dinitrosyl species generated on the cations with higher ionic charge numbers show absorption bands at higher wavenumbers. These results strongly support the above assignment, i.e., the anionic dinitrosyl species on Cu/ZSM-5. In fact, as shown in the later section, Cu^{2+} did not give the dinitrosyl species but Cu^+ did, substantiating the conclusion.

The infrared study of NO adsorbed on copper ion-exchanged Y zeolite was reported by Naccache et al.[22] They attributed the bands at 1918 cm^{-1} to $\nu(NO)^{\delta+}$ in the $Cu^{(2-\delta)+}$–$NO^{\delta+}$ complexes. This was further confirmed by the ESR study of Kasai and

TABLE II: Infrared Frequencies and Calculated Bond Angles for Dinitrosyl Species Adsorbed on Various Supports

dinitrosyl species	ν_{sym}, cm^{-1}	ν_{asym}, cm^{-1}	∠N–M–N, deg	ref
$Cu(NO)_2$/ZSM-5 zeolite	1827	1734	103	this work
$Rh(NO)_2$/Y zeolite	1860	1780	94[a]	31
	1848	1771	96[a]	32
$Fe(NO)_2$/Y zeolite	1917	1815	145[a]	19
$Co(NO)_2$/Y zeolite	1910	1830	123	20
$Co(NO)_2(NH_3)$/Y zeolite	1880	1800	123	20
$Rh(NO)_2/Al_2O_3$	1825	1743	120	33
$Mo(NO)_2/Al_2O_3$	1817	1713	104	34
	1810	1710	102–97	16
	1807	1700	116–105	35
$Cr^{III}(NO)_2/SiO_2$	1875	1745	135.2	38

[a] Calculated from the published spectra.

Bishop.[39] If one considers that the band wavenumber of 1906 cm^{-1} is close to 1918 cm^{-1}, the band at 1906 cm^{-1} can be assigned to $\nu(NO)^{\delta+}$.

The bands at 2238 and 2125 cm^{-1} in Figure 1b are probably attributed to N_2O and NO_2^+, respectively, formed by the reaction of NO based on the report of Chao and Lunsford.[40] Furthermore, these assignments were confirmed by the infrared spectra of N_2O and NO_2 adsorbed on Cu-MFI-112 in separate experiments. Here, the band at 1964 cm^{-1} remained unassigned: The band may be assignable to $(Cu)_n$–$NO^{\delta+}$ [41] since it appeared at higher wavenumber than that (1906 cm^{-1}) of the band attributable to Cu–$NO^{\delta+}$.

Adsorption Sites for the Respective NO Adsorbates. When the sample was cooled to room temperature in an oxygen atmosphere after the standard pretreatment, the admittance of NO resulted in the appearance of some absorption bands such as Cu–$NO^{\delta+}$ (1906 cm^{-1}) in a similar manner to Figure 1b but hardly yielded the bands of Cu–$NO^{\delta-}$ (1813 cm^{-1}) and Cu–$(NO)_2^{\delta-}$ (1827 and 1734 cm^{-1}). This indicates the absence of active sites for the adsorption of NO molecules with a negative charge after the oxidation treatment. On this sample, furthermore, there was no change in the band intensities with time, differing from that shown in Figure 6. The introduction of NO onto the sample wafer reevacuated at elevated temperature gave an infrared spectrum including the Cu–$NO^{\delta-}$ and Cu–$(NO)_2^{\delta-}$ bands, which was essentially the same as in Figure 1b. It follows that the appearance of $NO^{\delta-}$ and $(NO)_2^{\delta-}$ species requires desorption treatment of oxygen from the copper ion-exchanged zeolite at higher temperature, since it is already established that oxygen adsorbates on Cu-MFI can desorb at above 573 K.[42]

In a separate experiment, the state of copper on Cu-MFI-112 after various treatments was investigated by means of ESR and phosphorescence spectroscopy. After Cu-MFI-112 as-prepared was evacuated at room temperature, the ESR signal attributable to hydrated Cu^{2+} ions[43] was observed, while no phosphorescence spectrum due to Cu^+ ions[44] was detected. With the increment of evacuation temperature, the intensity of Cu^+ signal increased, while that of Cu^{2+} signal decreased. The observation suggests that the copper ion exchanged into zeolite was reduced to Cu^+ from Cu^{2+} by the treatment at elevated temperatures. Further, the admittance of NO after the CO adsorption on pretreated Cu-MFI resulted in the appearance of only two bands at 2154 and 1896 cm^{-1} (Figure 5). The band at 2154 cm^{-1} is clearly due to the Cu^+–CO complex, as has previously been reported in zeolite Y.[45] The intense band at 1896 cm^{-1} can be attributed to $NO^{\delta+}$. The slight shift to lower wavenumber from 1906 cm^{-1} (Figure 1b) would be due to some interaction between copper and CO such as the electron donation of CO to the copper ion. A similar shift was reported for the cobalt–silica catalyst.[46] In this experiment, no bands attributable to $NO^{\delta-}$, $(NO)_2^{\delta-}$, N_2O, and NO_2 were observed. The ESR, phosphorescence, and CO preadsorption experiment conclude that Cu^+ ion is active for the formation of the anionic mono- and dinitrosyl species, while Cu^{2+} ion is the site for the adsorption of $NO^{\delta+}$ species.

Decomposition Mechanism of NO on Cu-MFI. The interesting point in the infrared measurement is the change in the peak intensities with adsorption time as shown in Figures 6 and 7. The intensities of $NO^{\delta-}$ and $(NO)_2^{\delta-}$ species decreased, while that of $NO^{\delta+}$ species increased. These changes indicate the progress of the surface reaction even at room temperature, because the infrared measurements were performed in the presence of gaseous NO; that is, the decrease in the $NO^{\delta-}$ band was not attributable to the evacuation. In fact, it was confirmed in Figure 8 that the progress of the surface reaction yielded nitrogen and nitrous oxide molecules in the gas phase. In addition, when the oxidized or CO-preadsorbed Cu-MFI was exposed to NO at room temperature, only $NO^{\delta+}$ species was detected and the production of N_2 and N_2O was hardly observed. These results suggest that N_2 and N_2O are produced through $NO^{\delta-}$ and/or $(NO)_2^{\delta-}$ species.

From the decrement of the band intensities of $NO^{\delta-}$ and $(NO)_2^{\delta-}$ species as shown in Figures 6 and 7, one can directly measure the reaction rates of these surface intermediates. As shown in Figure 7, the intensities of bands at 1813 and 1734 cm^{-1} reached the constant values after the 870-min exposure to 52 Torr of NO. This indicates that the inert $NO^{\delta-}$ and $(NO)_2^{\delta-}$ species exist on Cu-MFI-157. Therefore, the absorbances of reactive $NO^{\delta-}$ and $(NO)_2^{\delta-}$ species responsible for the production of N_2 and N_2O, I_{react}, were estimated as follows:

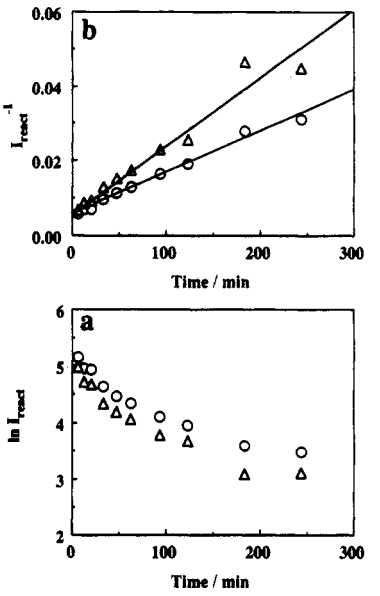

Figure 9. (a) First-order and (b) second-order plots of the disappearance of I_{react}. ○, 1813; △, 1734 cm^{-1}. P_{NO} = 52 Torr. Catalyst, Cu-MFI-157.

$$I_{react} = I_{obs} - I_{fin} \quad (3)$$

where I_{obs} is the band intensity observed and I_{fin} is that at t = 870 min. On the basis of eq 3, the intensity changes of the bands attributable to the reactive $NO^{\delta-}$ or $(NO)_2^{\delta-}$ species were plotted according to the first-order (eq 4) and second-order (eq 5) rate

$$\ln I_{react} = \ln I_0 - kt \quad (4)$$

$$1/I_{react} = 1/I_0 + kt \quad (5)$$

equations as shown in parts a and b of Figure 9, respectively, where t is the adsorption time, I_0 is the intensity at t = 0, and k is the rate constant. The linear correlation was observed in Figure 9b, but not in Figure 9a, showing that I_{react} decreased according to the second-order rate equation. The dependence concludes that the decomposition reaction does not proceed via the intramolecular reaction of one dinitrosyl species but does via intermolecular reaction between two neighboring adsorbed $NO^{\delta-}$ and $(NO)_2^{\delta-}$ species.

The sum of the intensities of the bands at 1813 and 1734 cm^{-1} at t = 0 (denoted by I_0^*) depended on the exchange level of copper ion. The dependence is shown in Figure 10a. I_0^* was the extrapolated value in Figure 9b. I_0^* increased little at lower exchange level, sharply increased at the exchange level of 30–50%, and gradually increased above 50%. The dependence was quite similar to those of the catalytic activity shown in Figure 10b, which is Figure 3 in ref 3, supporting that $NO^{\delta-}$ and $(NO)_2^{\delta-}$ species are intermediates and that Cu^+ ions are active sites for NO decomposition.

In Figure 11, the amounts of $NO^{\delta+}$ species at various adsorption times are plotted as a function of the total amounts of $NO^{\delta-}$ and $(NO)_2^{\delta-}$ species, based on the results in Figure 7. One can recognize the fine lineality between these amounts, which reveals that the increase in the intensity of the $NO^{\delta+}$ band is correlated with the decrease in those of the anionic adsorbed species. In other words, new adsorption sites for the $NO^{\delta+}$ species are produced through the surface reaction of the $NO^{\delta-}$ and $(NO)_2^{\delta-}$ species at room temperature. The disagreement between the increment of $NO^{\delta+}$ and the decrement of $NO^{\delta-}$ and $(NO)_2^{\delta-}$ in the figure is attributable to the difference of absorption coefficients of the respective species.

SCHEME I: Surface Reaction Mechanism

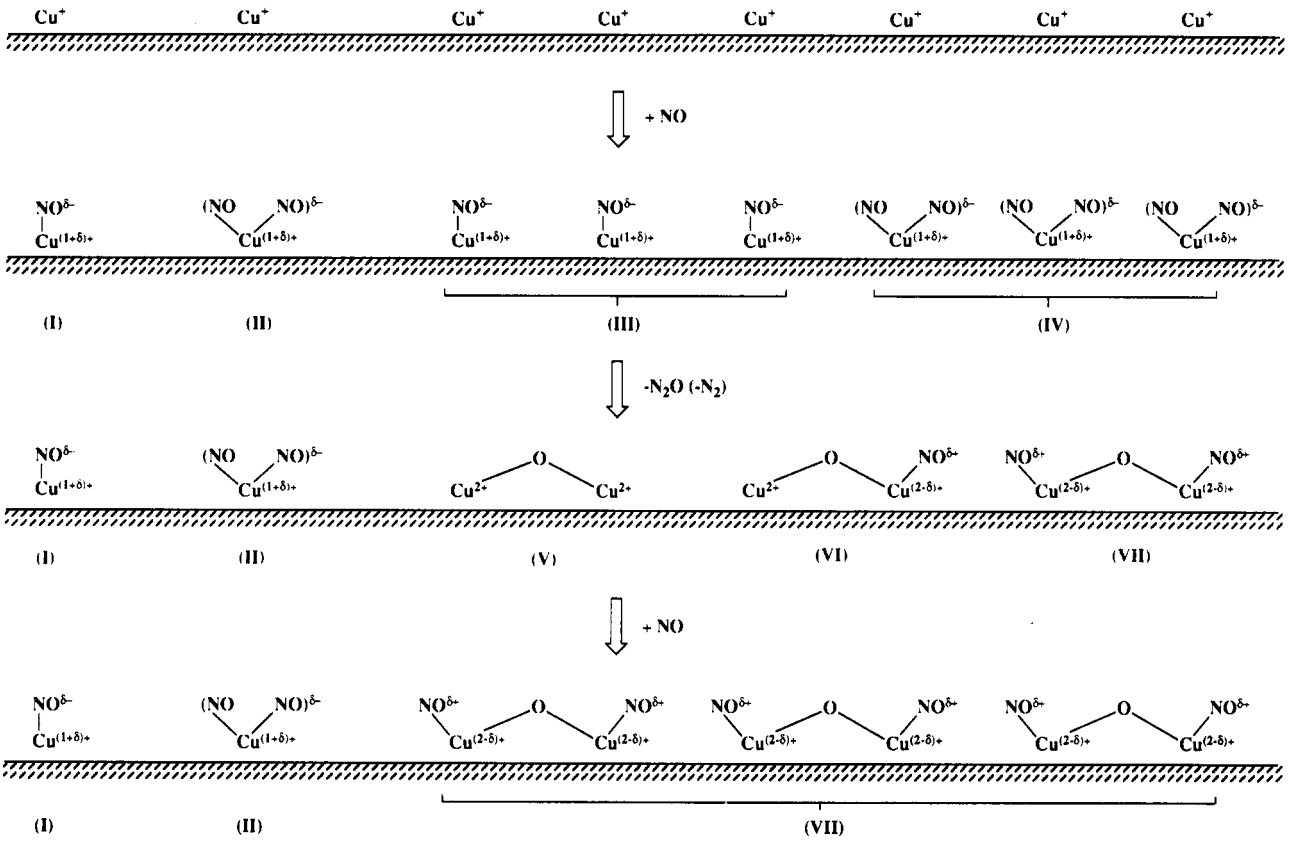

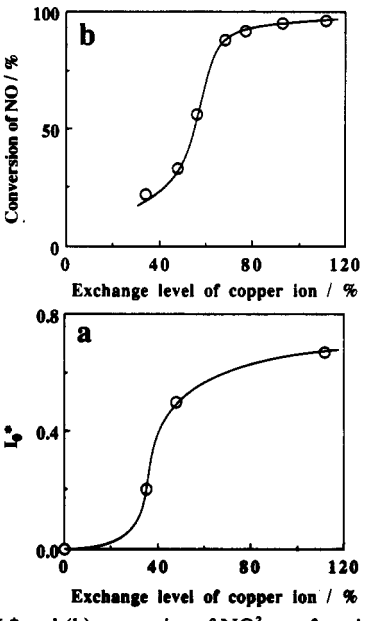

Figure 10. (a) I_0^* and (b) conversion of NO^3 as a function of exchange level of copper ions. (a) P_{NO} = 40 Torr. (b) Temperature = 723 K. W/F = 4.0 g s cm^{-3}. P_{NO} = 1.0%.

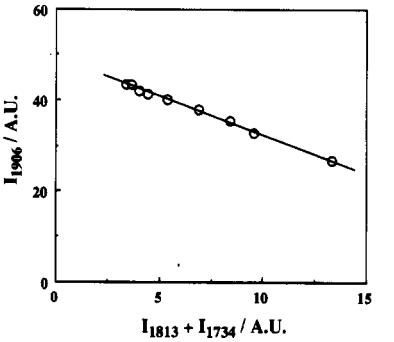

Figure 11. Correlation between I_{1906} and $I_{1813} + I_{1734}$. P_{NO} = 52 Torr. Catalyst, Cu-MFI-157.

The above findings and discussion lead to the following scheme, where Cu^{2+} ions existing after the standard pretreatment and $NO^{\delta+}$ formed just after the introduction of NO were excluded. Species I and II are the inert $NO^{\delta-}$ and $(NO)_2^{\delta-}$ species, respectively (Scheme I). After pretreatment at 773 K, Cu^+ ions are generated and act as active sites for the adsorption of $NO^{\delta-}$ or $(NO)_2^{\delta-}$ (I, II, III, and IV). These species can react with $NO^{\delta-}$ and $(NO)_2^{\delta-}$ molecules adsorbed on the neighboring Cu^+ site even at room temperature to yield N_2 and N_2O in the gas phase. The oxygen species remain on the surface and oxidize Cu^+ into Cu^{2+} (V, VI, and VII). The resulting Cu^{2+} further adsorbs NO as $NO^{\delta+}$ (VII). Finally, species I, II, and VII remain on the zeolite surface at room temperature.

The rate of formation of N_2 and N_2O at room temperature decreased with time as shown in Figure 8. This is due to the decrement of active sites by the adsorption of oxygen generated through the surface reaction. The presence of the remaining oxygen and their desorption above 573 K have already been confirmed.[42] Above 573 K, the regeneration of the active sites by the desorption of oxygen makes it possible to continue the catalytic decomposition cycle. In fact, the catalytic decomposition of NO becomes vigorous above 623 K.[2]

The nature of the active sites, in particular the presence of paired or neighboring copper ions, remains undetermined. Although the detailed study on the characterization of copper ions is in progress on ZSM-5 zeolites, Cu–O–Cu species in Y zeolites[47-49] and the species

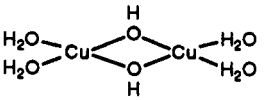

in mordenite zeolites[50] have been found, supporting Scheme I.

Acknowledgment. This work was supported by Grants-in-Aid for Scientific Research from the Ministry of Education, Science and Culture of Japan, and Nissan Science Foundation. We

acknowledged Mr. H. Takeda for experimental assistance.

Registry No. NO, 10102-43-9.

References and Notes

(1) Iwamoto, M.; Yokoo, S.; Sakai, K.; Kagawa, S. *J. Chem. Soc., Faraday Trans. 1* **1981**, *77*, 1629.
(2) Iwamoto, M.; Yahiro, H.; Mine, Y.; Kagawa, S. *Chem. Lett.* **1989**, 213.
(3) Iwamoto, M.; Yahiro, H.; Tanda, K.; Mizuno, N.; Mine, Y.; Kagawa, S. *J. Phys. Chem.* **1991**, *95*, 3727.
(4) Li, Y.; Hall, W. K. *J. Phys. Chem.* **1990**, *94*, 6415; *J. Catal.* **1991**, *129*, 202.
(5) Shimada, H.; Miyama, S.; Kuroda, H. *Chem. Lett.* **1988**, 1797.
(6) Teraoka, Y.; Fukuda, H.; Kagawa, S. *Chem. Lett.* **1990**, 1.
(7) Yasuda, H.; Mizuno, N.; Misono, M. *J. Chem. Soc., Chem. Commun.* **1990**, 1094.
(8) Hamada, H.; Kintaichi, Y.; Sasaki, M.; Ito, T. *Chem. Lett.* **1990**, 1069.
(9) For example: Nakamoto, K. *Infrared and Raman Spectra of Inorganic and Coordination Compounds*, 3rd ed.; John Wiley & Sons: New York, 1978; p 295.
(10) Arai, H.; Tominaga, H. *J. Catal.* **1976**, *43*, 131.
(11) Solymosi, F.; Sárkány, J. *Appl. Surf. Sci.* **1979**, *3*, 68.
(12) Tanabe, K.; Ikeda, H.; Iizuka, T.; Hattori, H. *React. Kinet. Catal. Lett.* **1979**, *11*, 149.
(13) Fierro, J. L. G.; Agudo, A. L.; Tejuca, L. G.; Rochester, C. H. *J. Chem. Soc., Faraday Trans. 1* **1985**, *81*, 1203.
(14) Morrow, B. A.; Chevrier, J. P.; Moran, L. E. *J. Catal.* **1985**, *91*, 208.
(15) Platero, E. E.; Spoto, G.; Zecchina, A. *J. Chem. Soc., Faraday Trans. 1* **1985**, *81*, 1283.
(16) Caceres, C. V.; Fierro, J. L. G.; Lopez Agudo, A.; Blanco, M. N.; Thomas, H. J. *J. Catal.* **1985**, *95*, 501.
(17) Kung, M. C.; Kung, H. H. *Catal. Rev.* **1985**, *27*, 425.
(18) Wichterlová, B.; Tvaruzková, Z.; and Nováková, J. *J. Chem. Soc., Faraday Trans. 1* **1983**, *79*, 1573.
(19) Segawa, K.; Chen, Y.; Kubsh, J. E.; Delgass, W. N.; Dumesic, J. A.; Hall, W. K. *J. Catal.* **1982**, *76*, 112.
(20) Windhorst, K. A.; Lunsford, J. H. *J. Am. Chem. Soc.* **1975**, *97*, 1407.
(21) Kasai, P. H.; Bishop, R. J., Jr.; Mcleod, D., Jr. *J. Phys. Chem.* **1978**, *82*, 279.
(22) Naccache, C.; Che, M.; Taarit, Y. B. *Chem. Phys. Lett.* **1972**, *13*, 109.
(23) For example: Amirnazmi, A.; Boudart, M. *J. Catal.* **1975**, *39*, 383. Ibbotson, D. E.; Wittrig, T. S.; Weinberg, W. H. *Surf. Sci.* **1981**, *110*, 294; *111*, 149. Gorte, R. J.; Schmidt, L. D. *Surf. Sci.* **1981**, *109*, 367. Campbell, C. T.; Erth, G.; Segner, J. *Surf. Sci.* **1982**, *115*, 309. Fulmer, J. P.; Tysoe, W. T. *Langmuir* **1990**, *6*, 1229. Smith, G. W.; Carter, E. A. *J. Phys. Chem.* **1991**, *95*, 2327.
(24) For example: Chin, A. A.; Bell, A. T. *J. Phys. Chem.* **1983**, *87*, 3700. Pande, N. K.; Bell, A. T. *J. Catal.* **1986**, *97*, 137; **1986**, *98*, 7.
(25) Iwamoto, M.; Furukuwa, H.; Kagawa, S. In *New Development in Zeolite Science and Technology*; Murakami, Y., Iijima, A., Ward, J. W., Eds.; Elsevier: Amsterdam, 1986; p 943.
(26) Fyfe, C. A.; Thomas, J. M.; Klinowski, J.; Gobbi, G. C. *Angew. Chem., Int. Ed. Engl.* **1983**, *22*, 259.
(27) Bell, A. T. In *Vibrational Spectroscopy of Molecules on Surfaces*; Yates, J. T., Jr., Madey, T. E., Eds.; Plenum: New York, 1987; p 105.
(28) Nakamoto, K. *Infrared and Raman Spectra of Inorganic and Coordination Compounds*; 3rd ed.; John Wiley & Sons: New York, 1978; p 9.
(29) Dinerman, C. E.; Ewing, G. E. *J. Chem. Phys.* **1970**, *53*, 626.
(30) Cotton, F. A., Wilkinson, G. *Advanced Inorganic Chemistry*, 4th ed.; John Wiley & Sons: New York, 1980; p 697.
(31) Iizuka, T.; Lunsford, J. H. *J. Mol. Catal.* **1980**, *8*, 391.
(32) Arai, H. *Ind. Eng. Chem. Prod. Res. Dev.* **1980**, *19*, 507.
(33) Liang, J.; Wang, H. P.; Spicer, L. D. *J. Phys. Chem.* **1985**, *89*, 5840.
(34) Valyon, J.; Hall, W. K. *J. Catal.* **1983**, *84*, 216.
(35) O'Young, C. L.; Yang, C. H.; DeCanio, S. J.; Patel, M. S.; Storm, D. A. *J. Catal.* **1988**, *113*, 307.
(36) Arai, H. *Hyomen* **1976**, *14*, 434.
(37) Chao, C. C.; Lunsford, J. H. *J. Phys. Chem.* **1972**, *76*, 1546.
(38) Kuger, E. L.; Kodes, R. J.; Gryder, J. W. *J. Catal.* **1975**, *36*, 142.
(39) Kasai, P. H.; Bishop, R. J., Jr. *J. Phys. Chem.* **1973**, *77*, 2308.
(40) Chao, C. C.; Lunsford, J. H. *J. Am. Chem. Soc.* **1971**, *93*, 71.
(41) Lokhov, Y. A.; Davydov, A. A. *React. Kinet. Catal. Lett.* **1975**, *3*, 39.
(42) Iwamoto, M.; Yahiro, H.; Tanda, K. *Stud. Surf. Sci. Catal.* **1988**, *37*, 219. Iwamoto, M.; Nakamura, M.; Nagano, H.; Kagawa, S.; Seiyama, T. *J. Phys. Chem.* **1982**, *86*, 153.
(43) Richardson, J. T. *J. Catal.* **1967**, *9*, 178.
(44) Texter, J.; Stome, D. H.; Herman, R. G.; Killer, K. *J. Phys. Chem.* **1977**, *81*, 333.
(45) Huang, Y. Y. *J. Am. Chem. Soc.* **1973**, *95*, 6636.
(46) Niiyama, H.; Echigoya, E. *J. Catal.* **1975**, *38*, 238.
(47) Chao, C. C.; Lunsford, J. H. *J. Chem. Phys.* **1972**, *57*, 2890.
(48) Jacobs, P. A.; Beyer, H. K. *J. Phys. Chem.* **1979**, *83*, 1174.
(49) Iwamoto, M.; Nakamura, M.; Nagano, H.; Kagawa, S.; Seiyama, T. *J. Phys. Chem.* **1982**, *86*, 153.
(50) Kuroda, Y.; Kotani, A.; Maeda, H.; Morikawi, H.; Morimato, T.; Nagao, M. *J. Chem. Soc., Faraday Trans.* **1992**, *88*, 1583.

Pulse Photoreflectance Spectroscopy of a CdS Single-Crystal Electrode

Seiichiro Nakabayashi[†] and Akira Kira*

The Institute of Physical and Chemical Research (RIKEN), Wakoshi, Saitama 351-01, Japan
(Received: December 23, 1991; In Final Form: August 19, 1992)

The transient photoreflectance induced by a 6-ns laser pulse was measured for a cadmium sulfide single-crystal electrode in aqueous solution with 1 M sodium sulfite as a reducing agent. Though the electrode used was a single crystal, the photoreflectance spectrum obtained resembled EER spectra of low structural quality such as sputtered or painted thin films. The time evolution of the spectrum intensity agreed with that of the excitation pulse. The longest limit of the lifetime of the hole was 2 ns. The spectral change also revealed that the repeated laser irradiation produced cadmium oxide on the surface. These features indicate that the high density of photons by the laser irradiation accelerates the photo-electrochemical surface corrosion.

Introduction

Surface-localized charges on the semiconductor electrode shift the flat-band potential.[1-8] Under the potentiostatic condition, the shift induces the change in the electrostatic field in the space charge region of the electrode.[8-10] Since the optical absorption of the semiconductor depends on the field strength, which is known as the Franz–Keldysh effect,[11-13] the change in the charge must affect the reflectance spectrum of the electrode. On photoexcitation, the surface-localized charge can be caused by either the accumulation of the minority carriers on the edge of the band bending or charge trapping by surface states.

Recently, the photoreflectance spectrum due to the Franz–Keldysh transition induced by charges trapped in a surface state has been measured for a cadmium sulfide single-crystal electrode under the intensity modulation of a continuous laser beam.[8] The present experiments aimed to expand the time resolution into the shorter region for evaluating the lifetime of the photocreated hole on top of the valence band.

Experimental Section

The electrochemical setup was similar to that in a previous experiment.[8] The semiconductor electrode was a CdS single crystal purchased from Eagle-Picher Research laboratory, mounted in a Kel-F electrode holder. The surface area of the electrode was 0.8 cm^2. The Ohmic contact of the electrode was

[†] Present address: Department of Chemistry, Faculty of Science, Hokkaido University, N10W8, Sapporo, 060, Japan.

0022-3654/92/2096-9366$03.00/0